Terahertz paintmeter for noncontact monitoring of thickness and drying progress in paint film

Takeshi Yasui, Takashi Yasuda, Ken-ichi Sawanaka, and Tsutomu Araki

We propose a paintmeter for noncontact and remote monitoring of the thickness and drying progress of a paint film based on the time-of-flight measurement of the echo signal of a terahertz (THz) electromagnetic pulse. The proposed method is effectively applied to two-dimensional mapping of the painting thickness distribution for single-layer and multilayer paint films. Furthermore, adequate parameters for the drying progress are extracted from the THz pulse-echo signal and effectively applied to monitor the wet-to-dry transformation. The THz paintmeter can be a powerful tool for quality control of the paint film on the in-process monitoring of car body painting.

OCIS codes: 110.6960, 120.4290, 300.6270, 310.1620.

1. Introduction

The painting of industrial products such as car bodies is important for rust prevention, waterproofing, and color effect. Hence, strict quality control of the paint film by use of a paintmeter (a piece of test equipment used to measure painting thickness) is required to maintain these functions. An in-process paintmeter should meet the following requirements: (a) noncontact and remote measurement, (b) suitability for a variety of paint films and substrates, (c) high precision for thickness determination, (d) individual thickness determination for multilayered paint, (e) detailed mapping of thickness distribution, (f) detection of painting defect, and (g) monitoring of wet-to-dry transformation. However, commercially available thickness meters, including ultrasonic testing,[1] eddy-current testing,[2] and electromagnetic testing,[3] are based on contact measurement. Although such contact-type thickness meters with hand-held scanners are powerful tools for portable applications, they are not necessarily suited for in-process paint monitoring because they do not adequately meet the above requirements. The applicability of conventional thickness meters to the above requirements is summarized in Table 1. One possible method for noncontact and remote measurement is optical probing. However, colored paint film is usually opaque and causes strong scattering of visible and infrared light, resulting in decreased reliability of the measurement. Therefore, to our knowledge, few studies on optical thickness meters have reported successful results.[4] Furthermore, it is difficult to monitor the wet-to-dry transformation of the paint film in all the methods mentioned above.

In contrast, the ultrashort pulse of electromagnetic radiation in the teraherz (THz) pulse[5] frequency range, namely, a THz electromagnetic pulse, adds such features as deep penetration and low scattering. THz tomography is based on the time-of-flight measurement of the THz pulse echo. Because it serves as a remote, noninvasive probe, THz tomography has been attracting attention as a possible substitute for the invasive x rays and contact ultrasonic waves in the fields of nondestructive testing and biomedical measurements.[6,7] Since THz tomography can reveal internal structures, depending on the distribution of the group refractive index in a given sample, it also provides a high potential for use in the multifunctional paintmeter described above. Furthermore, if there is a distinct spectroscopic difference in the THz region between the wet and dry condition of a paint film, it will cause a temporal change of the THz pulse-echo signal depending on the degree of drying. In this paper we propose a new testing technique, called the THz paintmeter, that uses a THz pulse to measure the thickness and dryness of a paint film. After describing the basic performance of the THz paintmeter, we demonstrate two-dimensional (2D) mapping

The authors are with the Graduate School of Engineering Science, Osaka University, 1-3 Machikaneyama, Toyonaka, Osaka 560-8531, Japan. T. Yasui's e-mail address is t-yasui@me.es.osaka-u.ac.jp.

Received 22 March 2005; revised manuscript received 21 July 2005; accepted 25 July 2005.

0003-6935/05/326849-08$15.00/0

Table 1. Applicability of Conventional Thickness Meters

Requirements for In-Process Paintmeter	Ultrasonic Testing	Eddy-Current Testing	Electromagnetic Testing
Noncontact and remote measurement	No	No	No
Suitability for various paint films and substrates	Yes	Partially	Partially
High precision for thickness determination	Yes	Yes	Yes
Individual thickness determination for multilayered paint	Partially	No	No
Detailed mapping of thickness distribution	No	No	No
Detection of painting defect	No	No	No
Monitoring of wet-to-dry transformation	No	No	No

of the painting thickness distribution in single-layer and multilayer paint films, and we also perform monitoring of the wet-to-dry transformation of a paint film.

2. Principle

The principle of the THz paintmeter is shown in Fig. 1. Let us consider a single layer of paint on a substrate. The thickness and the group refractive index of the paint film are d and n_g, respectively [Fig. 1(a)]. When the THz pulse is incident to the painting surface, the pulses are reflected at the air–paint boundary [boundary (1)] and the paint–substrate boundary [boundary (2)] because of the discontinuity of the group refractive index. This discontinuity results in the development of successive echo pulses [Fig. 1(b)].

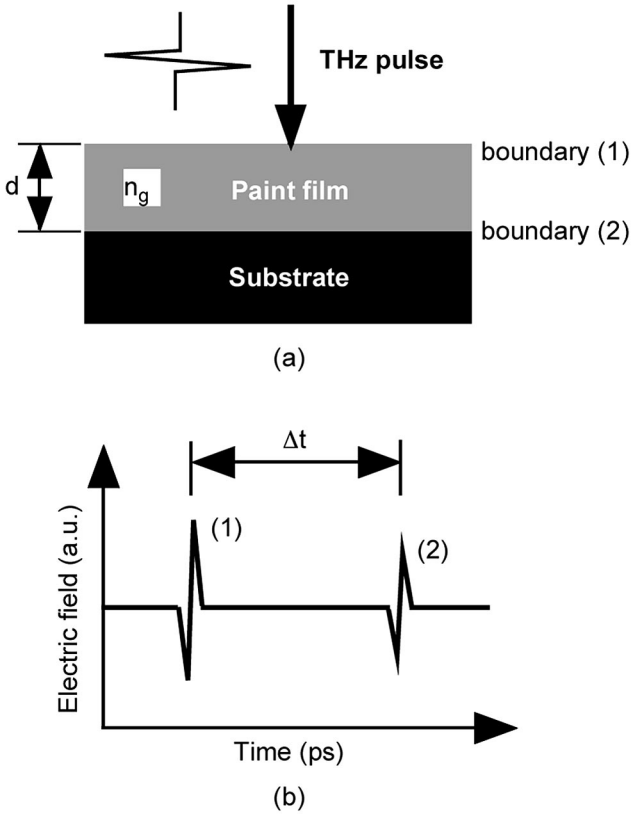

Fig. 1. Principle of the THz paintmeter. (a) Single-layer paint film and (b) temporal waveform of THz pulse echo.

The time delay (Δt) between two pulse echoes is given by

$$\Delta t = (2n_g d)/c, \tag{1}$$

where c is the velocity of light in a vacuum. Hence, assuming that the n_g value is a known constant in the frequency range of the spectrum of the THz pulse used in the measurements, we can determine the geometric thickness (d) through the measurement of Δt of the THz pulse echo. Such a principle can easily be extended to many types of paint films and substrates, multilayer paint films, wet paint films, or the 2D distribution of the painting thickness.

3. Experimental Setup

We used a THz tomography setup based on the reflection configuration shown in Fig. 2. The setup consists of a mode-locked Ti:sapphire (ML Ti:S) laser oscillator, photoconductive antenna (PCA) for THz generation, and free-space electro-optic sampling (FSEOS) for THz detection. Our laser is an 80 MHz ML Ti:S laser (Spectra-Physics, MaiTai). The laser pulse has a duration of 100 fs and an average power

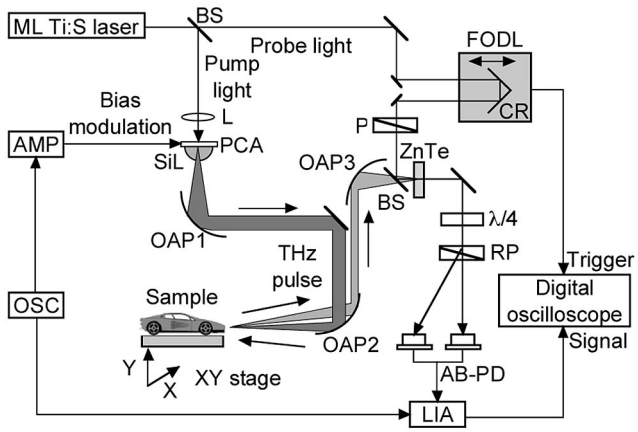

Fig. 2. Experimental setup. ML Ti:S laser, mode-locked Ti:sapphire laser; BS, beam splitter; L, lens; PCA, photoconductive antenna; SiL, hemispherical silicon lens; OAP1, OAP2, and OAP3, off-axis parabolic mirrors; ZnTe, zinc telluride crystal; FODL, fast optical delay line; CR, corner reflector; P, polarizer; λ/4, quarter-wave plate; RP, Rochon prism; AB-PD, autobalanced photoreceiver; LIA, lock-in amplifier; OSC, oscillator; AMP, amplifier.

Table 2. Basic Performance of the Present System

Pulse Width (ps)	Spectrum Bandwidth (THz)	Measurement Time (temporal waveform/s)	Signal-to-Noise Ratio	Spatial Resolution (mm)
0.4	0–2	1	100	1.7

of 1 W at 800 nm. The laser pulse is split into a pump beam and a probe beam with a beam splitter. The pump beam is focused onto a PCA with a lens (L), which was fabricated on low-temperature-grown GaAs with a bowtie length of 1 mm and a gap of 5 μm. To improve the signal-to-noise ratio in the FSEOS, we applied fast chopping of the THz pulse by electric bias modulation of the PCA.[8] The electric bias of the PCA is modulated in a unipolar sinusoidal wave with an appropriate offset (amplitude of 20 $V_{p\text{-}p}$, offset of 10 V, frequency of 100 kHz) by the combination of an oscillator and an amplifier. The resulting THz beam is focused on a sample via a hemispherical silicon lens, two off-axis parabolic mirrors (OAP1 and OAP2), and a plane mirror. For measurement of the painting thickness distribution, a 2D moving stage that scans the sample position laterally (*XY* stage) was adopted. The THz echo beam reflected on the sample is recollimated and focused onto a 1 mm thick (110) zinc telluride (ZnTe) crystal for the FSEOS sensor with two off-axis parabolic mirrors (OAP2 and OAP3). The effective focal lengths of OAP1, OAP2, and OAP3 are 76.2 mm. On the other hand, the probe beam via a fast optical delay line (FODL, APE, Scan Delay, stroke length of ±11.5 mm, scan rate of 1 Hz, resolution <0.5% of actual scan range) and a polarizer (P) is incident to the ZnTe crystal collinear to the THz pulse by another beam splitter. When the THz pulse and the probe pulse are incident to the ZnTe crystal simultaneously, the electric field of the THz pulse causes transient birefringence in the probe light as an electro-optical Pockels effect. After passing through the ZnTe crystal, the birefringence change is converted into an amplitude change by balance-detection optics composed of a quarter-wave plate (λ/4) and a Rochon prism, and then the amplitude change is detected with an autobalanced photoreceiver (New Focus Inc., 2007-M, bandwidth of 125 kHz) and a lock-in amplifier (NF Corporation, 5610B, bandwidth of 200 kHz, time constant of 1 ms). The temporal waveform of the THz electric field is obtained by a sampling measurement using the FODL. Finally, analog output from the lock-in amplifier is measured by a digital oscilloscope triggered by the position signal of the FODL. The basic performance of the present system is summarized in Table 2.

4. Results

A. Thickness Measurement of a Single-Layer Paint Film

Two dry single-layer paint films on an aluminum (Al) plate were prepared as samples: quick-drying black acryl (BA) paint and white enamel (WE) paint for general use. We determined the delay time (Δt) between the first and the second echoes [see Fig. 1(b)] at each painting thickness for the BA and WE paints using the proposed system. The Δt value was calculated from the stage displacement of the FODL. The stage displacement is equivalent to the optical thickness of the paint film ($n_g d$). The painting thickness (geometric thickness d) was measured beforehand with a contact-type thickness meter (eddy-current type, precision of ±3% of the actual thickness). The behavior of the THz pulse in the paint film is shown in Fig. 1. Since the n_g value gives the spectroscopic characteristics of the paint, it is inherent in each paint. Hence, the difference of the n_g value between different paints changes the optical thickness at the same d value, resulting in the sample-dependent time delay. Figure 3 shows the relationship between the painting thickness d and the delay time Δt (or optical thickness $n_g d$). Since a linear relationship between the painting thickness and the optical thickness was confirmed for each sample, we performed the linear approximation of the data as $y = \alpha x$, where y is the optical thickness, α is the slope constant, and x is the painting thickness (geometric thickness). The calculated linear approximations are $y = 1.81x$ for BA paint (fitting error of $R = 0.996$) and $y = 2.61x$ for WE paint (fitting error of $R = 0.968$). Since the slope constant of the approximate curve indicates the group refractive index of the paint film, the n_g value was 1.81 for the BA paint and 2.61 for the WE paint. Conversely, if the group refractive index is known,

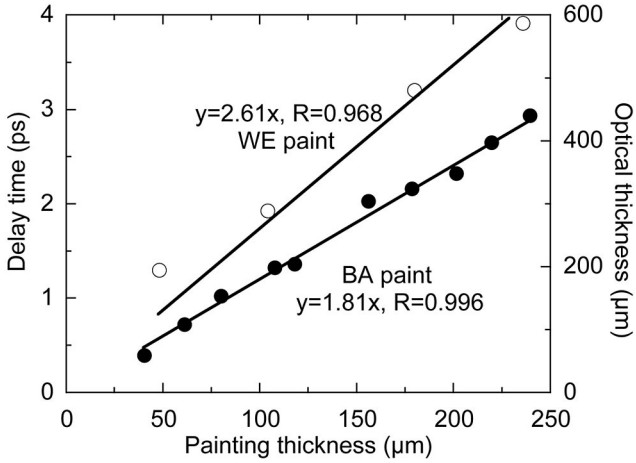

Fig. 3. Relationship between painting thickness and delay time of THz pulse echoes (or optical thickness). The solid lines were obtained from the linear approximation of the data as $y = \alpha x$, where y is the optical thickness, α is the slope constant (group refractive index), and x is the painting thickness (geometric thickness).

the painting thickness is determined by the precise measurement of the time delay. We here define the precision as the standard deviation of the differences of each measurement value from the value on the approximated curve. The resultant precision was 4 μm for BA, due to the nonlinearity of the FODL, the precision of the contact-type thickness meter, and/or the inconsistency of the measurement spot between the THz paintmeter and the contact-type thickness meter. Although the minimum painting thickness in Fig. 3 is 40 μm for BA and 48 μm for WE because of the limitations of sample preparation, the thickness resolution ($d_{\min}$) is determined from Eq. (1) as follows:

$$d_{\min} = (c\Delta T)/(2n_g), \tag{2}$$

where ΔT is the temporal width of the THz pulse (0.4 ps, see Table 2). The thickness resolution in the present system is estimated to be 30 μm for BA and 44 μm for WE. Work is in progress to improve this resolution by the application of a separation algorithm of superposed pulse echoes based on a linear optimization technique.

We next applied the THz paintmeter to several kinds of paint films actually used for car bodies. Table 3 summarizes the components of the resin and pigment used in these samples. The substrates of these samples are plates of galvanized sheet iron. To compare the performance of the paintmeter for noncontact measurement of painting thickness, we applied optical coherence tomography (OCT)[9] to all the samples. Another ML Ti:S laser (Femtolasers Produktions GmbH, FemtoSource sPRO, pulse duration of 9.5 fs, central wavelength of 780 nm, spectral width of 100 nm) was used as the laser source for the OCT. Figure 4 shows a comparison of the pulse-echo signal in the THz paintmeter and OCT for a metallic paint sample (sample C, thickness of 436 μm for the THz paintmeter and 103 μm for OCT). Two pulse-echo signals from the paint surface (air–paint boundary and paint–substrate boundary) were clearly observed in the THz paintmeter, whereas OCT detected only one pulse echo from the sample surface. In general, such a metallic paint film, with a pigment containing a lot of fine Al flakes (grain diameter of 10–25 μm, thickness of 0.3–0.4 μm), behaves as a multiple-scattering medium in the visible and infrared regions; however, in the THz region, the Al flakes hardly cause multiple scattering because of the relationship between the wavelength (≈300 μm) and the grain size. The applicability of the THz paintmeter and OCT for all samples is summarized in Table 3. From these results, one can confirm the advantage of the THz paintmeter for opaque paint films. We determined the group refractive index of each sample in the THz region in the same manner as for Fig. 3. The resulting n_g values are also shown in Table 3. Here, let us consider the difference in n_g values among these samples. There are differences in the n_g values among the four paint films (samples A, B, C, and D) comprised of a common resin (acryl–melamine) and

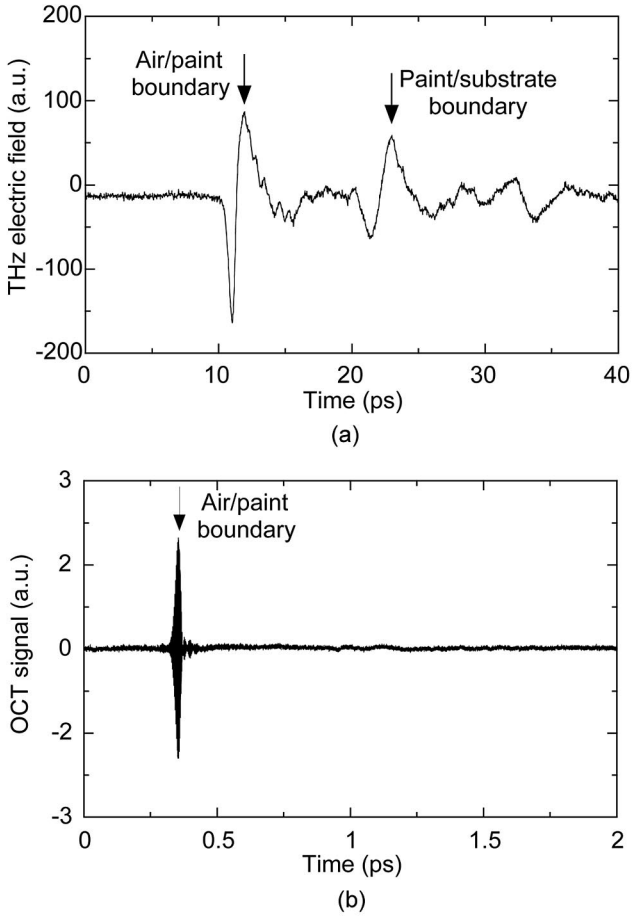

Fig. 4. Pulse-echo signal of a single-layer metallic paint film. (a) THz paintmeter and (b) OCT. The thickness of the paint film samples is 436 μm for the THz paintmeter and 103 μm for the OCT.

Table 3. Components of Resin and Pigment, Applicability of THz Paintmeter and OCT, and Group Refractive Indices in the THz Region with Respect to Five Kinds of Car Body Paints

			THz Paintmeter		
Sample	Resin	Pigment	Applicability	n_g	OCT Applicability
A	Acryl–melamine	None	Yes	1.50	Yes
B	Acryl–melamine	Mica	Yes	1.66	Yes
C	Acryl–melamine	Al flake	Yes	3.61	No
D	Acryl–melamine	Titanium oxide	Yes	2.01	No
E	Polyester–melamine	Titanium oxide	Yes	2.02	No

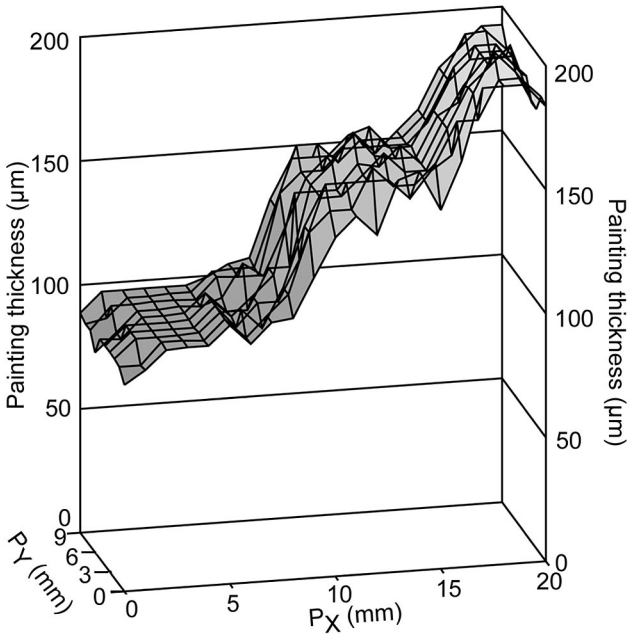

Fig. 5. Shown is the 2D distribution of the painting thickness for a single-layer WE paint film. P_X and P_Y indicate the X and Y coordinates of the sample position, respectively.

different pigments (none, mica, Al flake, and titanium oxide). On the other hand, no recognizable difference in n_g values was observed between the two paint films (samples D and E) comprised of different resins (acryl–melamine and polyester–melamine) and a common pigment (titanium oxide). Therefore we can conclude that the difference in the n_g values is mainly due to the pigment components. Also, such a difference in the n_g values implies a propagation mechanism of the THz pulse in the paint film. In samples B, D, and E, which contained the nonmetal pigment (mica or titanium oxide), the THz pulse could be transmitted through the paint film directly because of the excellent transmittance power to nonmetal pigments. As a result of the poor transmittance to metal pigments, the THz pulse in sample C, which contained the metal pigment (Al flake), was diffracted by the fine grains of the Al flake and then propagated through the paint film. Because of the resulting enlargement of the optical path length, the n_g value of sample C was larger than those of samples B, D, and E. From all these results, we conclude the validity of the THz paintmeter for actual car body paint.

It is of practical importance to extend the THz paintmeter to the distribution measurement of the painting thickness. Therefore we applied the proposed method to a single-layered WE paint film with a three-step surface on an aluminum substrate. The sample position was laterally scanned by the 2D moving stage at 1 mm/step within an area 9 mm $\times$ 20 mm. Figure 5 shows the 2D distribution of the painting thickness for the stepped sample, in which P_X and P_Y indicate the X and Y coordinates of the sample position, respectively (see Fig. 2). The painting thickness was calculated from the time-delay values at each point and the group refractive index of 2.61. The resultant painting thickness for each step is consistent with the values determined by the contact-type thickness meter (95, 145, and 200 μm). We can clearly perceive a detailed distribution of the painting thickness for each step as well as a blunt edge between adjacent steps.

B. Thickness Measurement of a Multilayer Paint Film

We extended the THz paintmeter to a multilayer paint film. It is difficult to determine the individual painting thickness for each layer with a conventional thickness meter. The prepared sample was a two-layer paint film. To evaluate the applicability to paint films on a nonmetal substrate, the same paints used in the previous experiment (BA and WE in Fig. 3) were layered on a polyethylene substrate (n_g = 1.80), as depicted in Fig. 6(a). The difference of the n_g values at the air–BA, BA–WE, and WE–substrate boundaries is approximately 0.8, resulting in the appearance of a THz pulse echo at each boundary. Figure 6(b) shows the impulse response signal of the THz echo-pulse train for the two-layer paint film based on numerical Fourier deconvolution.[7] Here the polarity and intensity of the impulse response signal depend on the difference of the n_g values across each boundary. The first positive echo pulse [(1)] and the second one [(2)] were generated from the air–BA and BA–WE boundaries, respectively. The third was a negative echo [(3)] generated from the WE–substrate boundary. In this way, pulse echoes from each boundary developed successively in the picosecond range, thus confirming that the time sequence profile of the pulse echoes depends on the internal structure of the two-layer paint film. In addition, we determined each thickness distribution for the two-layer paint film by scanning the sample laterally. Figure 6(c) shows the result of individual thickness distributions of the two-layer painted film calculated from the time delay and the n_g value. The observed uniformity of the thickness distribution was 239 $\pm$ 33 μm [(mean) $\pm$ (standard deviation)] and 158 $\pm$ 11 μm for the BA and WE layers, respectively. The lack of uniformity for the BA layer is obvious. From this result, we confirm that the proposed THz paintmeter is applicable to a multilayer paint film.

C. Detection of Paint-Off Area

One of the significant defects of paint film quality is the paint-off, which is the separation of the paint film from the substrate, because the substrate is highly subject to the corrosion resulting from moisture or salt penetration through the paint-off area of the coating. Such paint-off is caused by poor painting quality, unsuitable time for painting, contamination on the painting substrate, an undesirable surrounding for painting, and/or deterioration by aging. There is considerable need for nondestructive inspection of the paint-off area because it is difficult to detect it with the conventional thickness meter. In our next experiment, we tried to detect a paint-off area on a

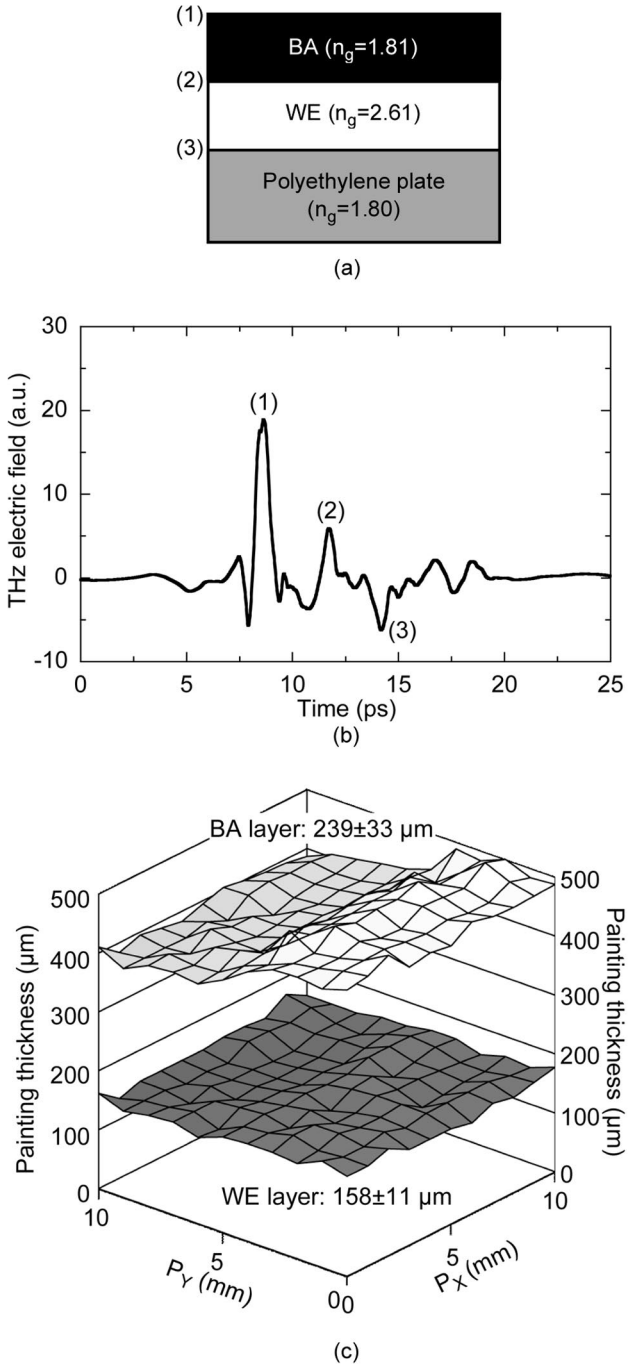

Fig. 6. Shown is the 2D distribution of painting thickness for a two-layer paint film on a nonmetal substrate. (a) Sample, (b) impulse response of the THz echo-pulse train, (c) 2D distribution of the individual painting thickness. The difference of the n_g values at the air–BA, BA–WE, and WE–substrate boundaries are approximately 0.8.

paint film. A single-layer WE painting on an aluminum substrate was prepared so that part of the painting separated from the aluminum substrate, as shown in Fig. 7(a). Two positive pulse echoes from the air–WE and WE–substrate boundaries were observed in the intact area. In contrast, the paint-off area appeared as a second negative pulse echo and a

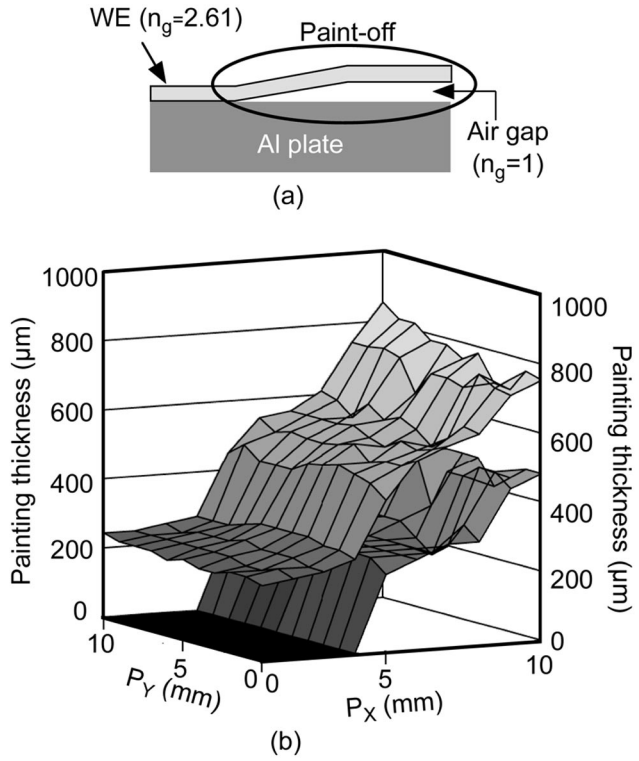

Fig. 7. Detection of the partial paint-off area. (a) Sample and (b) 2D distribution of the paint-off area. The paint-off area with the maximum air gap of 555 μm is observed within the area P_X = 2.5–10 mm.

third positive echo at the WE–air-gap and air-gap–substrate boundaries, respectively. Figure 7(b) shows the 2D distribution of the partial paint-off area calculated from the time delay and the group refractive indices of WE and air. We confirmed the paint-off area with the maximum air gap of 555 μm within the area P_X = 2.5–10 mm.

D. Monitoring of the Drying Process

Another advantage of our THz paintmeter is the noncontact and remote monitoring of a wet paint film. As an actual in-process control of the painting quality, monitoring of the paint drying condition is often required in addition to the thickness measurement. If there is a distinctive difference of the spectroscopic characteristics (index of refraction and/or absorption) in the THz range between the wet condition and the dry condition of the paint film, the wet-to-dry transformation will cause a temporal change of the THz pulse-echo train. In general, the drying process of acryl paint is temporally advanced by the volatilization of an organic solvent (e.g., paint thinner) added to the paint. The volatilization helps the transformation to the dry condition. In our previous paper, we confirmed the obvious difference of spectroscopic characteristics between the dry paint film and the wet one by THz time-domain spectroscopy.[10] The spectral change accompanying the wet-to-dry transformation results in attenuation, delay, and/or distortion of the THz pulse echoes. Therefore, in this

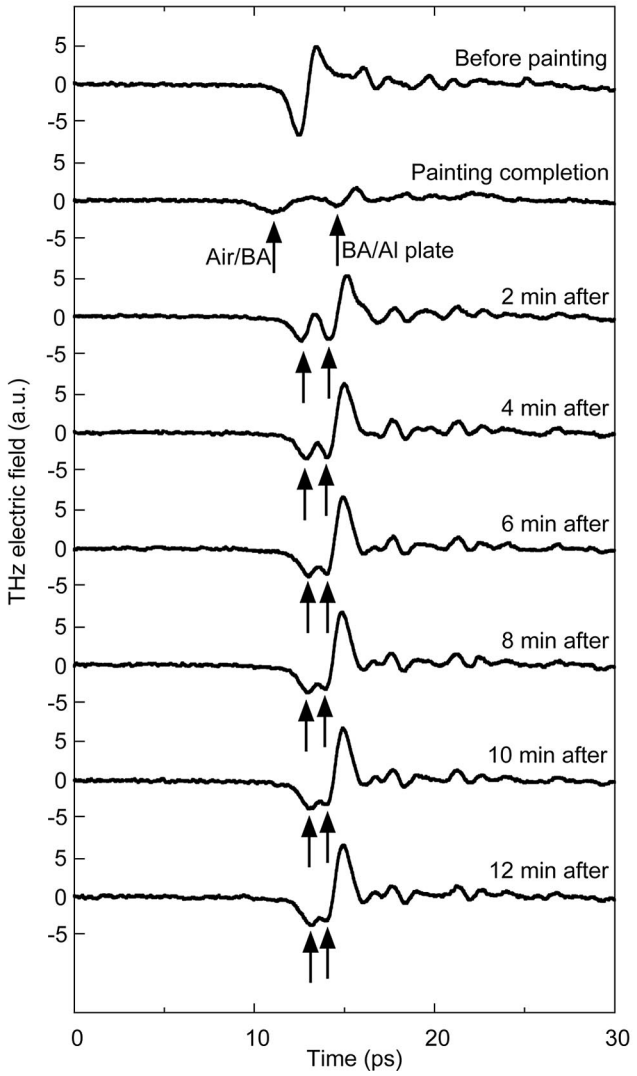

Fig. 8. Temporal evolution of a THz pulse-echo signal before and after painting. The drying process is almost completed after 10 min.

paper, we tried to monitor the wet-to-dry transformation of BA paint on an aluminum plate using a temporal profile of the THz pulse-echo signal. Figure 8 shows the temporal evolution of the THz pulse-echo signal before and after painting. Only one pulse echo from the air–substrate boundary was observed before painting, while two pulse echoes appeared after painting: The first echo came from the air–BA boundary and the second one from the BA–substrate boundary. The two echo pulses did not separate completely because the paint film was very thin with respect to the corresponding pulse width. These two pulse echoes temporally evolved in time delay and pulse height. For example, the time delay between the two pulse echoes decreased over time, whereas the height of each negative echo pulse increased over time. After 10 min, the temporal change was almost finished because of the quick-drying paint, implying completion of the drying process. To evaluate dryness, it is necessary to investigate whether any drying degree

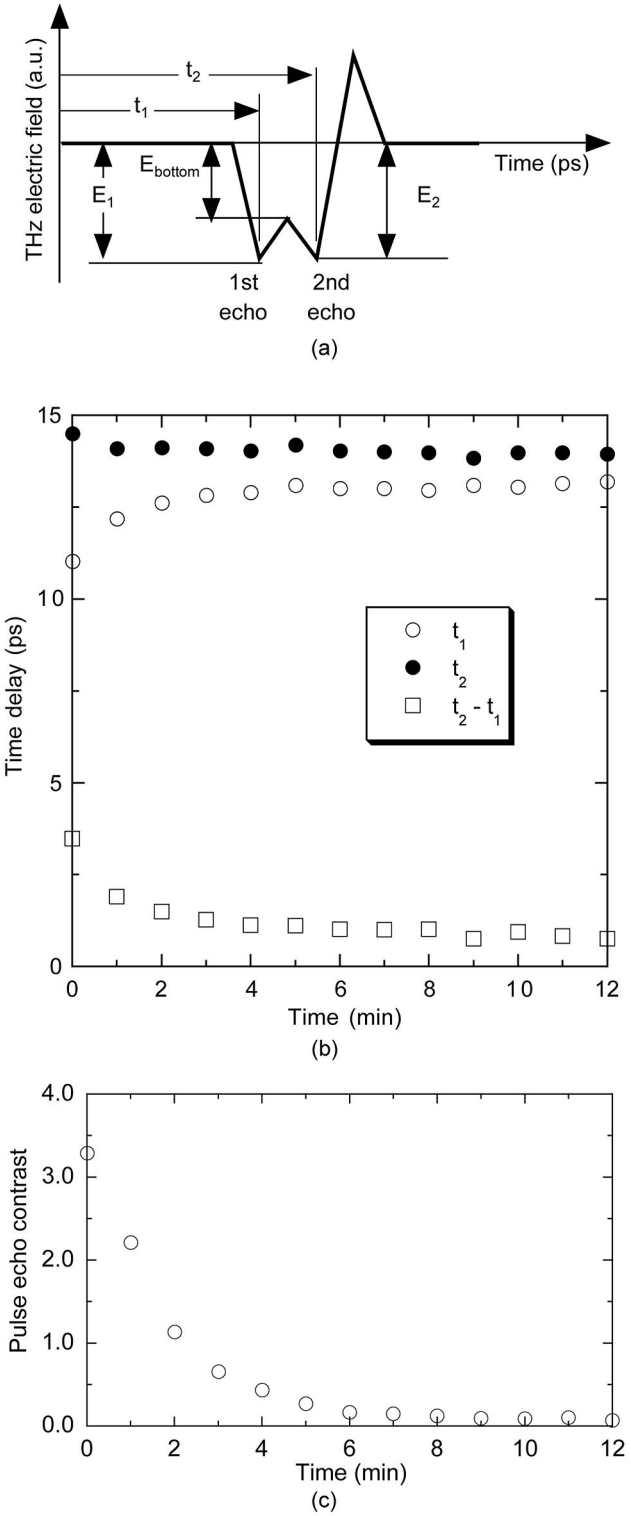

Fig. 9. Monitoring of the drying process. (a) Parameter of THz pulse-echo signal; (b) temporal change of t_1, t_2, and $(t_2 - t_1)$ values; (c) temporal change of pulse-echo contrast (PEC). The t_1, and $(t_2 - t_1)$ values relate to the geometric thickness and optical thickness of the paint film, respectively. The PEC value is defined as PEC $= (E_2 - E_{\text{bottom}})/(E_2 + E_{\text{bottom}})$.

parameters can be extracted from the observed waveform of the THz echo pulse in Fig. 8. The possible parameters extracted from the THz echo signal are

illustrated in Fig. 9(a). The first and second echo come from the paint surface and the paint–substrate boundary, and their times are t_1 and t_2, respectively. Hence, the t_1 value relates to the geometric thickness (d) of the paint film, whereas the $(t_2 - t_1)$ value relates to the optical thickness ($n_g d$) of the paint film. Figure 9(b) shows the temporal change of t_1, t_2, and $(t_2 - t_1)$ obtained from the pulse profiles shown in Fig. 8. The increase of the t_1 value indicates the physical shrinking of the wet paint film by the drying process. In contrast, the t_2 value remains almost constant, even when the t_1 value increases, resulting in a similar change of the $(t_2 - t_1)$ value to the t_1 value. This result implies that the decrease of the optical thickness is mainly due to the decrease of the geometric thickness caused by physical shrinking. Such a smooth decay curve with respect to the drying process reflects the wet-to-dry transformation in the paint film. Another dryness parameter is the height of the THz echo pulses. The characteristic changes of the temporal evolution in Fig. 8 include the height increase in the two negative pulse echoes [E_1 and E_2 in Fig. 9(a)] and the disappearance of the depression between them [E_{bottom} in Fig. 9(a)]. E_1 depends on the group refractive index of the painting surface, and hence reflects the degree of drying only near the painting surface. On the other hand, the E_2 value reflects the drying process of the whole paint film, and it is a result of the THz absorption in the whole paint film and the reflection at the air–BA and BA–substrate boundaries. We empirically defined the pulse-echo contrast, called PEC, as PEC = $(E_2 - E_{\mathrm{bottom}})/(E_2 + E_{\mathrm{bottom}})$. Figure 9(c) shows the temporal change of the PEC value with respect to the drying process. As one can see, the PEC value shows a smooth decay curve with respect to the drying process, and so this feature is suitable for monitoring the degree of drying in the painting.

5. Conclusion

We have proposed a THz paintmeter to monitor the thickness and degree of drying in a paint film based on THz tomography. The precision and resolution of the thickness determination of a single-layer paint film were 4 and 30 μm for BA paint, respectively. The proposed method is useful to determine the thickness of each layer in multilayer painting and can be extended to 2D mapping of the painting thickness distribution. The temporal change of the THz pulse echoes is effective to monitor the drying process of a paint film. For practicality, we proposed the PEC value, which is extracted from the temporal waveform of the THz echo pulse. This value is an indicator of the degree of drying in a thin paint film. From all the experiments, we conclude that the proposed THz paintmeter is a powerful tool for the measurement of the painting thickness and the drying progress in paint films. Furthermore, a rapid THz paintmeter combining real-time 2D THz tomography[11,12] or asynchronous optical sampling THz time-domain measurement[13] will open the door for in-process monitoring of the painting quality of car bodies and other painted products.

This work was supported by the Industrial Technology Research Grant Program in 2004 from the New Energy and Industrial Technology Development Organization of Japan, the Strategic Information and Communications R&D Promotion Programme from the Ministry of Internal Affairs and Communications of Japan, the Mazda Foundation, and the Suzuki Foundation. We are grateful to Takakazu Yamane at Mazda Motor Corporation and Mamoru Hashimoto at Osaka University for their productive discussions. We also thank Toshiyasu Mitsunari for his technical support in our experiments.

References

1. For example, see http://www.kett.co.jp/e/products/pro3/lu200.html.
2. For example, see http://www.kett.co.jp/e/products/pro3/lh200c.html.
3. For example, see http://www.kett.co.jp/e/products/pro3/le200c.html.
4. J. Ying, F. Liu, P. P. Ho, and R. R. Alfano, "Nondestructive evaluation of incident corrosion in a metal beneath paint by second-harmonic tomography," Opt. Lett. **25,** 1189–1191 (2000).
5. D. H. Auston, K. P. Cheung, and P. R. Smith, "Picosecond photoconducting Hertzian dipoles," Appl. Phys. Lett. **45,** 284–286 (1984).
6. D. M. Mittleman, R. H. Jacobsen, and M. C. Nuss, "T-ray imaging," IEEE J. Sel. Top. Quantum Electron. **2,** 679–692 (1996).
7. D. M. Mittleman, S. Hunsche, L. Boivin, and M. C. Nuss, "T-ray tomography," Opt. Lett. **22,** 904–906 (1997).
8. T. Yasui and T. Araki, "Dependence of terahertz electric field on electric bias and modulation frequency in pulsed terahertz emission from electrically-modulated photoconductive antenna detected with free-space electro-optic sampling," Jpn. J. Appl. Phys. **44,** 1777–1780 (2005).
9. D. Huang, E. A. Swanson, C. P. Lin, J. S. Schuman, W. G. Stinson, W. Chang, M. R. Hee, T. Flotte, K. Gregory, C. A. Puliafito, and J. G. Fujimoto, "Optical coherence tomography," Science **254,** 1178–1181 (1991).
10. T. Yasui, T. Mitsunari, and T. Araki, "Measurement of thickness and dry-state of the paint film using THz electromagnetic pulse," in *Abstract of the Ninth International Workshop on Femtosecond Technology*, M. Nakazawa, ed. (Femtosecond Technology Research Association, 2002), p. 182.
11. T. Yasui, T. Yasuda, and T. Araki, "Real-time two-dimensional terahertz tomography," in *Proceedings of the Joint 30th International Conference on Infrared and Millimeter Waves and 13th International Conference on Terahertz Electronics*, K. J. Button, ed. (IEEE, 2005), p. 580–581.
12. T. Yasuda, T. Yasui, T. Araki, and E. Abraham, "Real-time two-dimensional terahertz tomography for in-process terahertz paintmeter," submitted to Opt. Lett.
13. T. Yasui, E. Saneyoshi, and T. Araki, "Asynchronous optical sampling terahertz time-domain spectroscopy for ultrahigh spectral-resolution and rapid data acquisition," Appl. Phys. Lett. **87** 061101 (2005).